J Comput Aided Mol Des (2014) 28:443–454
DOI 10.1007/s10822-014-9724-4

Prediction of SAMPL4 host–guest binding affinities using funnel metadynamics

Ya-Wen Hsiao · Pär Söderhjelm

Received: 15 November 2013 / Accepted: 29 January 2014 / Published online: 18 February 2014

Abstract Accurately predicting binding affinities between ligands and macromolecules has been a much sought-after goal. A tremendous amount of resources can be saved in the pharmaceutical industry through accurate binding-affinity prediction and hence correct decision-making for the drug discovery processes. Owing to the structural complexity of macromolecules, one of the issues in binding affinity prediction using molecular dynamics is the adequate sampling of the conformational space. Recently, the *funnel metadynamics* method (Limongelli et al. in Proc Natl Acad Sci USA 110:6358, 2013) was developed to enhance the sampling of the ligand at the binding site as well as in the solvated state, and offer the possibility to predict the absolute binding free energy. We apply funnel metadynamics to predict host–guest binding affinities for the cucurbit[7]uril host as part of the SAMPL4 blind challenge. Using total simulation times of 300–400 ns per ligand, we show that the errors due to inadequate sampling are below 1 kcal/mol. However, despite the large investment in terms of computational time, the results compared to experiment are not better than a random guess. As we obtain differences of up to 11 kcal/mol when switching between two commonly used force fields (with automatically generated parameters), we strongly believe that in the pursuit of accurate binding free energies a more careful force-field parametrization is needed to address this type of system.

Keywords Funnel metadynamics · Binding affinity · CGENFF · GAFF · NAMD

Y.-W. Hsiao
CVMD Innovative Medicine, AstraZeneca, 431 83 Mölndal, Sweden
e-mail: Ya-Wen.Hsiao@AstraZeneca.com

P. Söderhjelm (✉)
Department of Theoretical Chemistry, Lund University, Chemical Center, P.O. Box 124, 221 00 Lund, Sweden
e-mail: par.soderhjelm@teokem.lu.se

Introduction

Accurate predictions of the binding affinities between ligands and biological macromolecules remain a challenge in many fields. Although some methods, e.g. free energy perturbation (FEP) [2], solves the statistical–mechanical problem rigorously, the computational costs are prohibitive for industrial applications. For the same reason, a proper assessment of FEP-predicted binding affinities across many (e.g., several hundreds) ligands is not available. Methods that may be of more practical use generally employ various approximations. Many tests have shown that the success or failure of these methods is system-dependent [3, 4, 5]. Therefore there is no generally applicable method for calculating accurate binding affinities to date. For methods based on molecular dynamics (MD), the two major remaining problems are inaccurate force fields and inadequate sampling of the conformational space. The force field problem is particularly troublesome for general compounds (i.e. molecules not included in the original parametrization of the force field), because the force field parameters of general compounds typically need to be set without reference to experimental data. For the sampling problem, owing to the structural complexity of bio-macromolecules, numerous conformations and binding possibilities need to be explored by the MD simulations, and therefore it is difficult to adequately sample all the important states of the system.

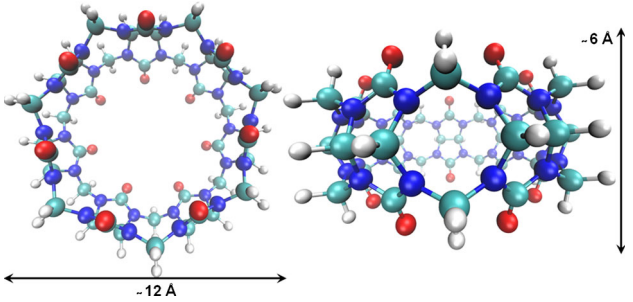

Fig. 1 Top-view (*left panel*) and side-view (*right panel*) of the host CB7

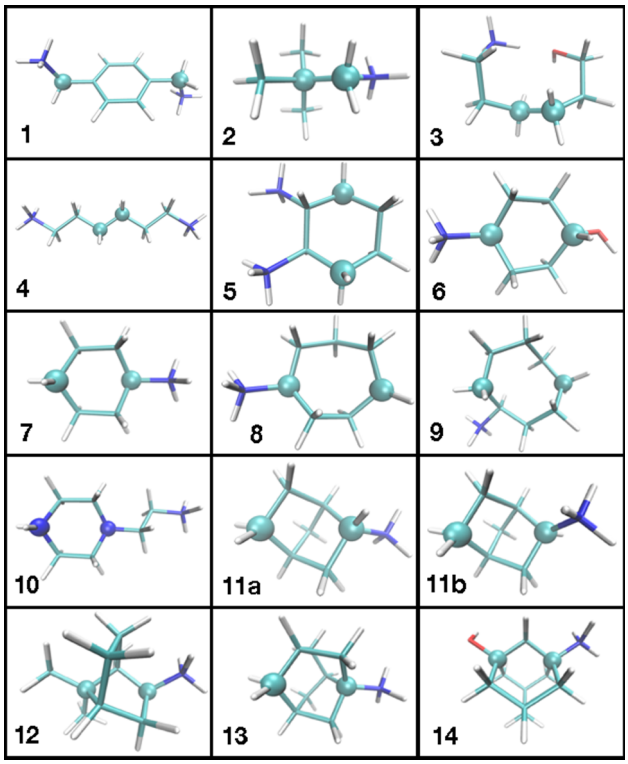

Fig. 2 The SAMPL4 guest molecules. The two atoms marked as *balls* were the ones used to define the molecular axis

Metadynamics [6] is among the emerging techniques for studying protein–ligand binding [7, 8, 9]. The method is especially useful when the exact binding pose is not known or when the binding is accompanied by conformational changes in the protein [10, 11]. However, the method suffers from the problem that once the ligand leaves the binding site, it has difficulties to find its way back. Therefore, a specialized metadynamics method for ligand binding, funnel metadynamics (FM), has been developed [1]. By applying a funnel-shaped restraint potential stemming out from the binding site, it reduces the space to explore in the unbound state and thereby enhances the sampling along the binding path. FM presents a possibility to accurately predict the absolute protein–ligand binding free energy, hence more tests of its performance are of great interest.

The SAMPL4 host–guest binding blind challenge provides valuable model systems for understanding protein–ligand binding, as these two types of systems are governed by the same type of interactions. The structural complexity is much lower in host–guest systems than in proteins, thus allowing for more thorough tests. In addition, the blind aspect of the challenge ensures that the predictive capability of any method employed becomes known regardless of its performance; thus the SAMPL4 challenge offers a fair comparison of the methods.

In this study, we perform a systematic evaluation of the FM method by computing binding affinities between cucurbit[7]uril (CB7) (Fig. 1) and 14 guest molecules (Fig. 2). We find that the method is robust with respect to the choice of funnel parameters and that it gives well-converged results for moderate simulation times. However, the results are very dependent on the choice of the force field.

Methods

System setup

The host (CB7) and guest molecule were solvated in a cubic box of TIP3P water [12], with side length approximately 49 Å, together with one to two chloride ions to neutralize the system; both steps were done using the modeling facilities of VMD [13]. Force-field parameters were taken from CGENFF [14], version 0.9.6 beta, which assigns parameters by analogy with molecules in the CHARMM force field. For some guest molecules, additional calculations were performed using the General Amber force field (GAFF) [15] for both the host and the guests, with partial charges determined by restrained ESP fitting (RESP) [16] at the Hartree–Fock level in vacuum using the 6-31G* basis set, on structures optimized at the B3LYP level [17, 18] using the 6-31G** basis set [19, 20, 21] and including aqueous solvation effects with the polarizable continuum model [22] implemented in Gaussian 09 [23].

MD simulations in the NPT ensemble at 300 K and 1 atm were carried out using Langevin dynamics as implemented in the NAMD [24] program, with a time step of 2 fs and a damping coefficient of 1 ps^{-1}. The pressure was controlled by the Nosé–Hoover Langevin piston method with an oscillation period of 100 fs and a decay time of 50 fs. The particle mesh Ewald method [25] was used for treating electrostatics in our periodic systems, with the grid size 50 × 50 × 50 and fourth-order interpolation. The non-bonded cutoff distance was 10 Å.

In contrast with the experimental situation, most systems were simulated without salt. However, salt-containing systems were simulated for guest molecules **1** and **2** in order to assess the Coulomb screening effects and the competition in binding by metal ions. The experimental work was done in the presence of 0.1 M Na_3PO_4, but we substituted it with 0.3 M NaCl (to avoid multivalent ions), thus keeping the same concentration of Na^+ ions. With the size of our water box, 18 NaCl units made the concentration 0.3 M.

The PLUMED plugin [26] (version 1.3) was used together with NAMD to perform the funnel metadynamics. The center of mass of the host was loosely restrained to the center of the box (to avoid technical problems with the periodic boundaries), but no other restraints were used. The simulation times for each ligand were all longer than 90 ns and up to 450 ns in order to check the convergence of the binding free energy estimate.

The protonation states of the guest molecules were assigned by ACD/pKa [27]. All amine groups were protonated except the tertiary amine in molecule **10**; thus we modeled this molecule as a divalent (and not trivalent) cation.

Funnel metadynamics

To provide a local frame of reference, we defined the z axis as being perpendicular to the CB7 ring plane with the origin at the center of mass of the host. This axis is not related to any of the periodic box vectors, because the host is free to rotate. Two collective variables (CVs) were defined for the metadynamics: The first CV (CV1) is the projection of the center of mass of the guest onto the z axis. The second CV (CV2) is the difference between the projections of two selected atoms of the guest (marked in Fig. 2) onto the z axis, divided by the maximum distance between the points. Thus, for guests with a rigid ring structure, it represents the cosine of the angle θ between the guest axis and the z axis, as shown in Fig. 3.

The geometry of the funnel restraint potential is shown in Fig. 3. Owing to the symmetry of the CB7 host, we used a double-sided funnel potential stemming out to the bulk from either side of the host along the z-axis. Using the notation of Ref. [1], the following parameters were used: $z_{cc} = 11$ Å, $R_{cyl} = 1$ Å, and $\alpha = 35°$ (these parameters are defined in Fig. 3). More precisely, if $R_f(z)$ is the radius of the funnel at a given z, the restraint potential for the guest at a center-of-mass distance r from the z axis equals

$$V_f(r,z) = \begin{cases} \kappa\left[r - R_f(z)\right]^2, & \text{if } r > R_f(z) \\ 0, & \text{otherwise} \end{cases} \quad (1)$$

where $\kappa = 5$ kcal/(mol Å^2). To prevent the guest from moving out of the periodic box (which would not make sense as the funnel restraint is not aligned with the box vectors), a steep repulsive wall was added at $|z| > 21$ Å.

Both one- and two-dimensional (1D and 2D) metadynamics simulations were performed, the former using only CV1 and the latter both CV1 and CV2. The purpose of CV1 is to enhance the movement of the guest going in and out of the binding site and to provide a suitable CV along which to compute the potential of mean force (PMF). Moreover, the repeated movement of the guest into solution also enhances the sampling of the guest's torsional degrees of freedom, because the flexibility is greater in the unbound state. The purpose of CV2 is to promote the rotation of the guest molecule to facilitate entering and exiting the binding site. Because we saw a tendency in the 1D simulations for the ligand to get temporarily stuck in one orientation and on one side of the host, we focus on the 2D simulations in this report.

Gaussian functions with a height of 0.1 kcal/mol were deposited every 0.5 ps, with widths 0.3 Å and 0.01–0.1 (depending on the rigidity of the molecule and determined from the fluctuations in unbiased MD) along CV1 and CV2, respectively. To ensure a smooth convergence, we used the well-tempered formulation of metadynamics [28]. The speed of decreasing the amount of added bias potential during the simulation was controlled by a ΔT of 9,300 K. This unusually high bias temperature allows us to

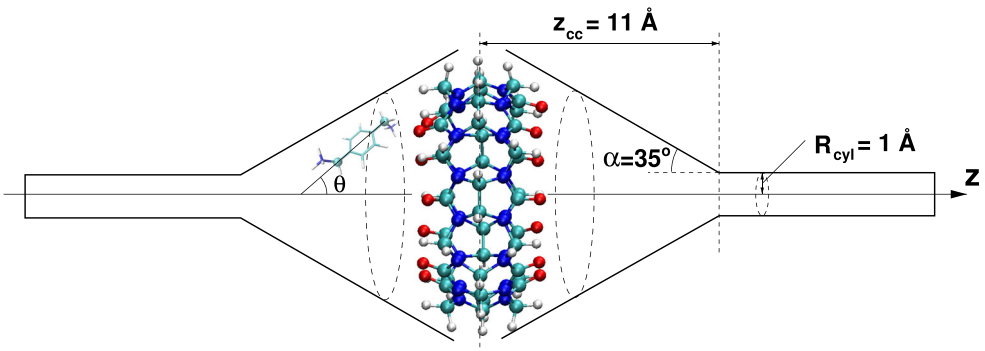

Fig. 3 Geometry of the double funnel restraint used in the FM simulations. Some test calculations used $R_{cyl} = 2$ Å but otherwise the same parameters. The definition of the angle θ, used to construct the second collective variable, $\cos\theta$, is also shown for guest molecule **1**

overcome free-energy differences of more than 20 kcal/mol (estimated in preliminary simulations), while continuing to smooth out the free-energy surface (FES) at a reasonable speed (because 33 % of the height remains when the bias potential is 20 kcal/mol).

The binding free energy estimation

The binding free energy was estimated as follows. First, the 2D free energy surface was projected down on CV1 (z axis) using a Boltzmann averaging over CV2 at a temperature of 300 K. The reconstruction of the free energy surface and the projection were both done using the sum_hills utility provided with the PLUMED plugin [26].

As discussed in Ref. [29], the binding free energy ΔG_{bind} is related to the one-dimensional PMF $w(z)$ through

$$e^{-\beta\Delta G_{bind}} = C^0 S^* e^{\beta\Delta G_a^{site}} \int_{site} dz e^{-\beta[w(z)-w(z^*)]} \quad (2)$$

where $C^0 = 1/1660$ Å^{-3} is the standard concentration, S^* is the effective cross-sectional area swept by the ligand restrained along the z axis, ΔG_a^{site} is the free energy for restraining the bound ligand along the axis, and $\beta = (k_B T)^{-1}$ where k_B is Boltzmann's constant and T is the absolute temperature. In our case, the restraint does not affect the bound ligand due to its funnel shape, so $\Delta G_a^{site} = 0$. Moreover, owing to the steep shape of V_f, we assume that the ligand motion in the unbound state is restricted to the flat region, so that $S^* = \pi R_{cyl}^2$. These are the same assumptions as done in Ref. [1].

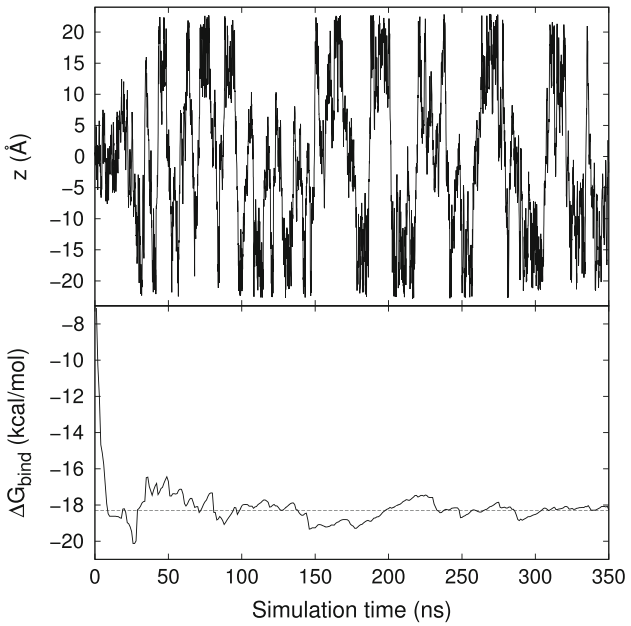

Fig. 4 Trajectory of the (refined) FM simulation of molecule **1**. *Upper panel* shows the projection of the ligand on the z axis as a function of simulation time. *Lower panel* shows the estimated binding free energy as a function of simulation time, with the dashed line representing the reported result

On evaluating Eq. 2, we define the *site* as $|z| < 6$ Å to include possible secondary minima (although their contribution is always negligible; using instead $|z| < 2$ Å affected the result by less than 0.01 kcal/mol for all molecules). The reference level of the PMF, $w(z^*)$, corresponding to the unbound state, was evaluated as the average $w(z)$ over the range $14 \leq |z| \leq 20$ Å. Shifting the lower limit of this range between 12 and 16 Å affected the result by less than 0.1 kcal/mol for all molecules. The ΔG_{bind} obtained from Eq. 2 was monitored regularly for convergence, as exemplified in Fig. 4. A time average of the last 100 ns of the simulation was taken as the reported binding free energy.

An estimate of the sampling error (i.e. the error caused by insufficient sampling) is computed as the maximum of three contributions:

- the standard deviation of the time fluctuation of the last 50 ns of the convergence curve (cf. Fig. 4).
- the drift (fluctuations at a longer timescale) in the convergence curve, estimated as the difference between the averages obtained for the last 50 ns of the simulation and for the 50 ns preceding the last 50 ns.
- the left–right asymmetry of the one-dimensional PMF, i.e. the difference between the binding free energy evaluated using a $w(z^*)$ averaged on $z < -14$ Å and $z > 14$ Å, respectively.

The reason for using the maximum, instead of a more typical error propagation rule, is that these three error contributions are not independent; in contrast the error caused by left–right asymmetry is typically also reflected in the time fluctuations. Finally, it should be noted that our error estimate would not include contributions from conformational states that are not sampled in the simulations. By running long simulations with a methodical enhanced-sampling strategy, we minimize the risk of overlooking such states.

Results and discussion

For each guest molecule in the data set, we performed a well-tempered funnel metadynamics (FM) simulation using two collective variables (CVs): the projection of the center of mass of the ligand on the z axis, and the orientation ($\cos\theta$) of the ligand relative to the z axis (cf. Fig. 3).

At convergence, the simulations give us the two-dimensional FES of the system. This surface is then projected down to a one-dimensional potential of mean force (PMF), from which the binding free energy is computed as described in the "Methods" section. The PMF of each

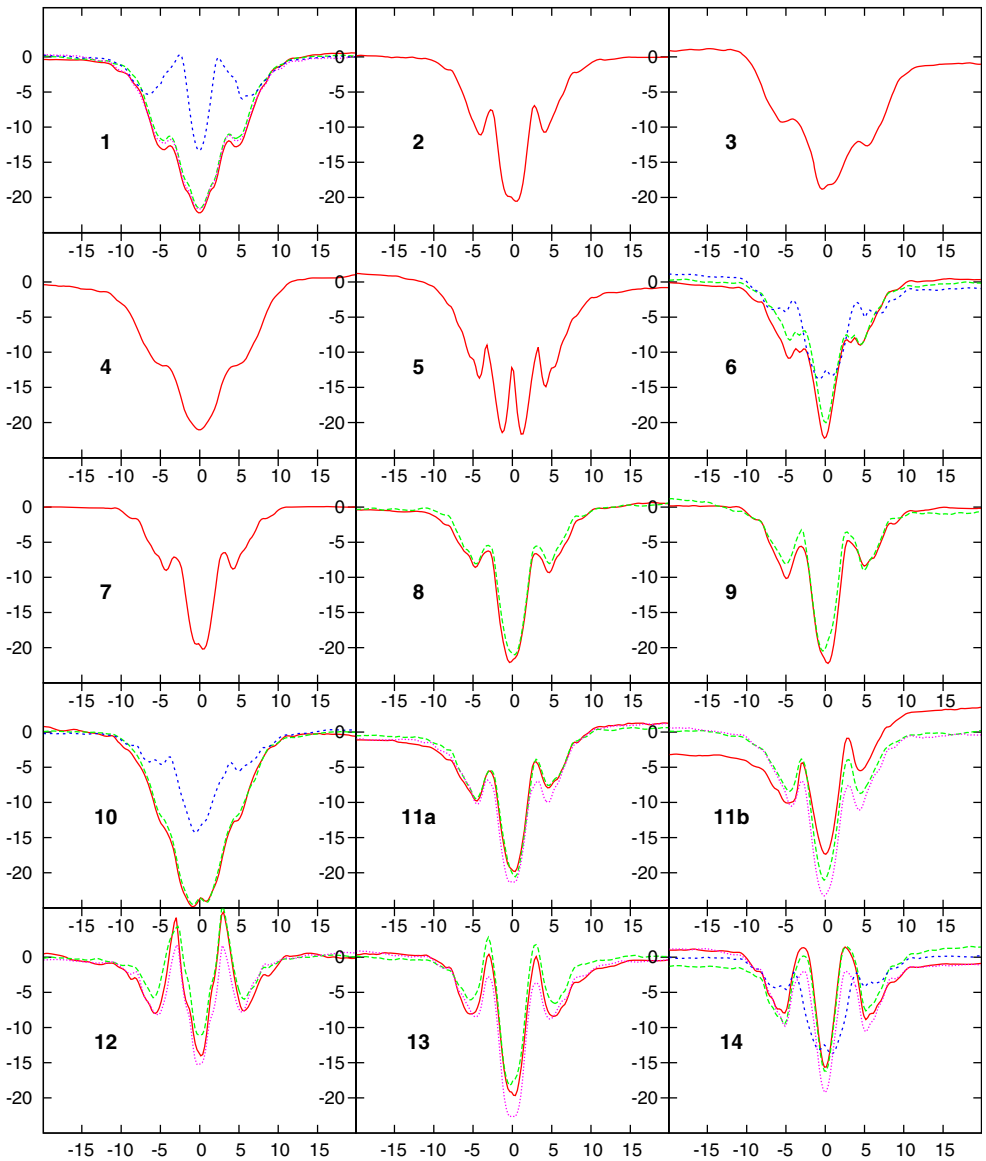

Fig. 5 Potential of mean force projected onto the z axis for all molecules, calculated with CGENFF (refined; *red solid line*), CGENFF with $R_{cyl} = 2$ Å (*green dashed line*), GAFF (*blue short-dashed line*), or CGENFF with modified charges (*magenta dotted line*)

guest molecule is shown in Fig. 5 and the estimated binding free energies are given in Table 1. For some of the molecules, the PMF was evaluated with various choices of parameters, as is discussed in subsequent sections.

We give two sets of results in Table 1: the data we submitted for the SAMPL4 blind prediction (original) and our current estimate with the same model (refined). The difference between the original and refined results comes from slightly longer simulation times for some molecules and an improved evaluation of Eq. 2 that gives an almost constant contribution of $\sim$1 kcal/mol. Together, these improvements makes the absolute prediction slightly worse but affects the relative prediction by less than 2 %.

Free-energy surfaces for illustrative molecules

The time evolution of a typical FM simulation (for guest **1**) is shown in Fig. 4. During the 350 ns of simulation, the guest molecule passes through the binding site (at $z = 0$) more than 30 times, each time refining the energy landscape slightly. The lower panel shows the convergence of the estimated binding free energy from the same simulation. For most molecules, the result is converged to within 1 kcal/mol after 100–200 ns.

The resulting FES is shown in Fig. 6 together with a typical snapshot of the bound complex. The FES has some interesting features. First, we note that the landscape flattens out outside the host so that a well-defined $w(z^*, \cos\theta)$ is obtained (for

Table 1 Experimental and calculated binding free energies in kcal/mol for the SAMPL4 molecules binding to CB7

Mol	Exp.	Original	Refined	Funnel sens.
1	−9.9	−17.5 ± 0.5	−18.3 ± 0.8	−0.3
2	−9.6	−15.7 ± 0.7	−16.8 ± 0.2	N/A
3	−6.6	−12.6 ± 0.9	−12.8 ± 1.1	N/A
4	−8.4	−16.4 ± 0.5	−17.8 ± 0.7	N/A
5	−8.5	−16.9 ± 0.8	−17.5 ± 0.7	N/A
6	−7.9	−17.5 ± 0.4	−18.3 ± 1.1	0.0
7	−10.1	−16.4 ± 0.6	−16.8 ± 1.1	N/A
8	−11.8	−17.6 ± 0.8	−17.8 ± 1.0	−0.8
9	−12.6	−17.8 ± 1.0	−17.8 ± 0.7	0.2
10	−7.9	−20.0 ± 0.5	−21.1 ± 0.4	−0.6
11a	−11.1[a]	−14.8 ± 0.6	−15.7 ± 0.9	−0.6
11b		−15.3 ± 2.5	−15.7 ± 3.6	−1.8
12	−13.3	−10.0 ± 2.2	−11.3 ± 2.6	0.8
13	−14.1	−14.5 ± 1.0	−15.7 ± 0.5	0.5
14	−11.6	−11.3 ± 0.6	−12.2 ± 0.7	0.1
AE		−5.31	−6.07	
AUE		5.93[b]	6.46	
AUE_o		3.07[c]	3.02	

Originally submitted predictions and refined values are given, as well as the sensitivity to the funnel restraint (*funnel sens.*), defined as the difference between a FM calculation using $R_{cyl} = 2$ Å and the (refined) FM calculation using $R_{cyl} = 1$ Å. The average error (AE), average unsigned error (AUE), and average unsigned error after subtraction of the average error (AUE_o) are also given

[a] Racemic mixture

[b] 5.77 if molecule **1** is excluded

[c] 3.14 if molecule **1** is excluded

convenience all FES have been shifted by an irrelevant constant so that $w(z^*, \cos\theta) = 0$). Second, we see that there is symmetry around both axes. This is because this particular guest molecule is symmetric. In general, the landscape should have inversion symmetry, i.e. $w(z, \cos\theta) = w(-z, -\cos\theta)$, because mirroring the molecule's position and orientation recovers the same system owing to the symmetric structure of the host (cf. Fig. 3). Consequently, the one-dimensional PMF should also be symmetric, i.e. $w(z) = w(-z)$. Note that this symmetry is not enforced in any way during the simulations, so the fulfillment of inversion symmetry can be taken as an indication of the statistical accuracy of the method.

Third, we see that there is a large high-energy region around the origin. This region corresponds to configurations with the ligand inside the host, but with the ligand axis lying almost perpendicular to the z axis, as shown in Fig. 6. For this big ligand, the host has to distort significantly (changing the length to width ratio to $\sim$ 1.7) to accommodate such ligand poses. Moreover, there is a huge cost of desolvating both the positively charged amino groups. Therefore, the hypothetical free-energy barrier height for rotating the guest at $z = 0$ is larger than 36 kcal/mol (the very maximum is too high to be sampled at our choice of bias temperature).

Monovalent guest molecules have smaller rotational barriers, e.g., 12 kcal/mol for molecule **13**, which is analyzed in Fig. 7. For this molecule, we also see a secondary binding pose with a well-depth of 11 kcal/mol. This pose corresponds to a loose complex with polar interactions between the guest and the carbonyl oxygens of the host. Similar minima of varying depths are seen for all of the guest molecules, but they do not contribute to the binding free energy at the studied temperature.

A very different-looking FES is obtained for molecule **5** (cf. Fig. 8). For this molecule, the molecular axis is defined in such a way (cf. Fig. 2) that it prefers an orientation perpendicular to the z axis. Again, the molecule can reside at two different positions along the z axis, giving the two types of poses depicted in Fig. 8.

Overall accuracy

A key purpose of this study is to determine what accuracy one can expect for the FM method. We divide the errors into sampling errors, stemming from imperfect sampling, and model errors stemming from the imperfect force field and modeled system. Our main objective is to reduce the sampling errors to such an extent that the remaining discrepancy with experiment comes from the model alone. However, to directly estimate the sensitivity of the results

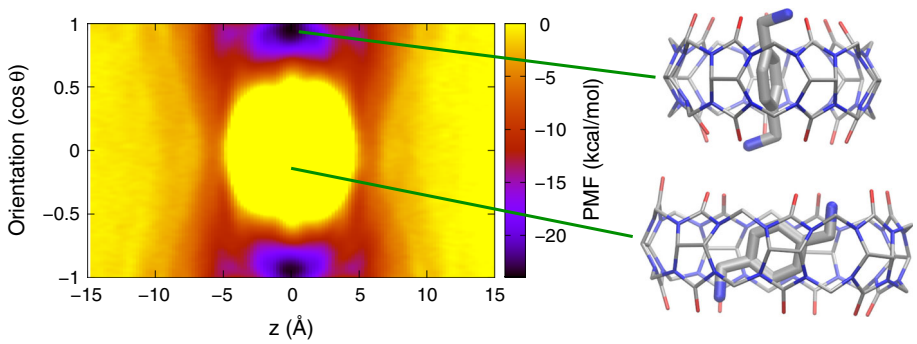

Fig. 6 Two-dimensional free-energy surface for molecule **1** and typical configurations corresponding to the free-energy minimum (*top*) and the high-energy region (*bottom*)

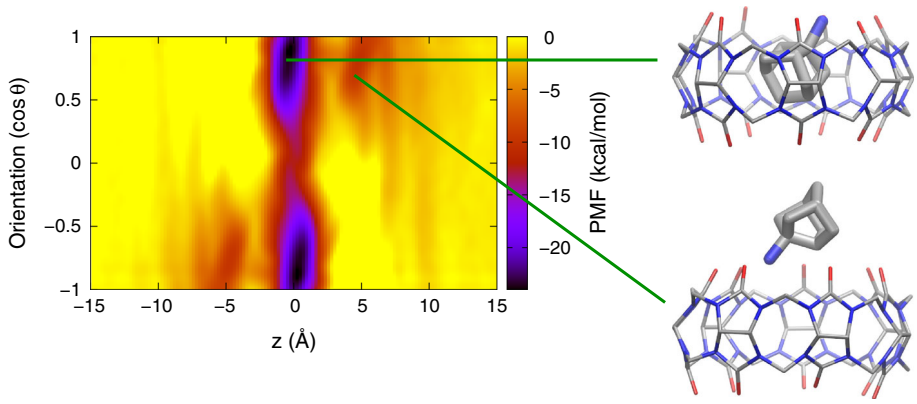

Fig. 7 Two-dimensional free-energy surface for molecule **13** and typical configurations corresponding to the free-energy minimum (*top*) and a secondary minimum (*bottom*)

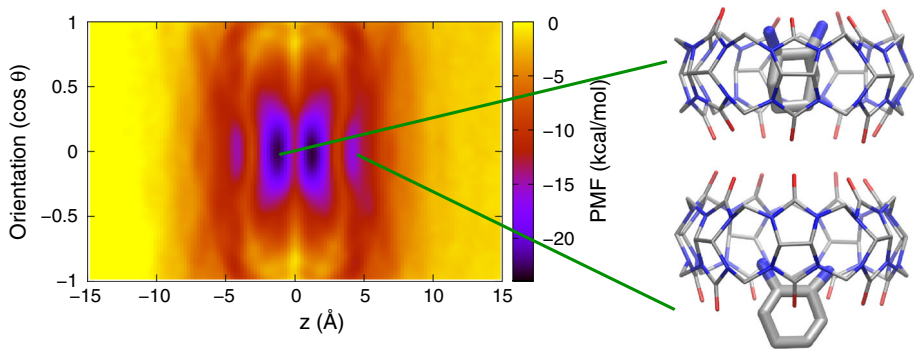

Fig. 8 Two-dimensional free-energy surface for molecule **5** and typical configurations corresponding to the free-energy minimum (*top*) and a secondary minimum (*bottom*)

to the force field, we also investigate some force field modifications in "Dependence on the force field" section.

An estimate of the sampling error for each FM calculation is given in Table 1. It is computed as the maximum of three contributions: the time fluctuation and drift of the convergence curve (cf. Fig. 4) and the left–right asymmetry of the PMF, as described in the "Methods" section (the last contribution was not included in the originally submitted uncertainties). The three contributions are similar in magnitude and rather correlated (with a correlation coefficient $R^2 = 0.5$ for all three combinations), but the left–right asymmetry is usually the largest contribution, whereas the drift and fluctuation are both below 0.6 kJ/mol for all but three molecules.

For most molecules, the sampling error is around 1 kcal/mol, but for the most "well-behaved" molecules, the error is significantly smaller, e.g., 0.2 kcal/mol for molecule **2**. Two molecules have significantly larger error: molecule **11b** (3.6 kcal/mol) and molecule **12** (2.6 kcal/mol). As we noticed problems with the charges, we did not run these simulations until convergence but instead focused on the simulations with modified charges (see below).

Another possible source of sampling error in these simulations is the funnel restraint (cf. Fig. 3). Therefore, for ten of the molecules we performed an additional FM calculation, in which we used a larger radius ($R_{cyl} = 2$ Å) for the cylindrical part of the funnel restraint. After adjusting the S^* factor in Eq. 2, this calculation should give identical result as the standard calculation using $R_{cyl} = 1$ Å. Indeed, as shown in Table 1, the difference is well within the statistical uncertainty for all molecules (for **11b** the large-radius result is the better estimate with a sampling error of only 0.5 kcal/mol). This indicates that the FM results are insensitive to the choice of R_{cyl} within a reasonable range. Most likely, this conclusion holds for other funnel parameters as well, so that one can choose the parameters with only efficiency considerations, as long as the funnel restraint does not affect the bound ligand.

Comparison to experiment

The experimental values [30] are also given in Table 1. The average unsigned error (AUE) of the refined *absolute binding affinities* is 6.5 kcal/mol (5.9 kcal/mol for the original submission), which is a very high error. The task given for this part of the SAMPL4 challenge was instead to predict *relative binding affinities* (in fact, the experimental affinity of guest **1** was available before the challenge [31] although it was not used in this study). When subtracting the average signed error (−6.1 kcal/mol), our results have an average unsigned relative error (AUE_o) of 3.0 kcal/mol (3.1 kcal/mol for the original submission).

This error is still large and there is no correlation between the experimental and calculated results, as shown

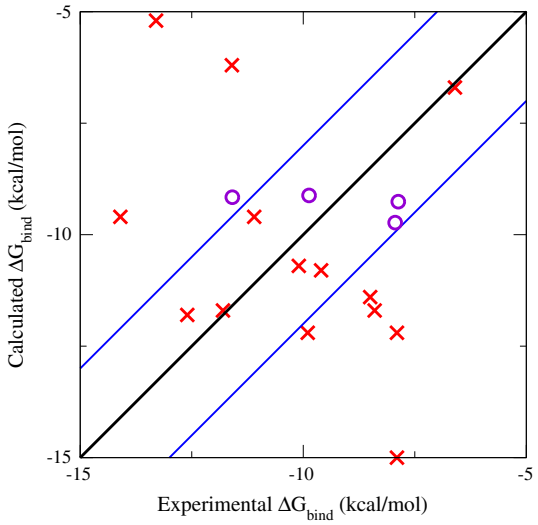

Fig. 9 Comparison between the calculated and the experimental relative binding free energies using CGENFF (*crosses*) and GAFF (*rings*). To depict relative free energies, the average difference between the calculated and experimental values for the two sets (−6.5 and −0.7 kcal/mol, respectively) has been subtracted from the calculated binding free energies. The *blue lines* indicate a range within 2 kcal/mol from the experimental results

in Fig. 9. Consequently, the original submission is only ranked 13th among the 20 submissions to the SAMPL4 challenge by AUE_o, and it has the worst correlation coefficient and ranking ability among all submissions, despite being one of the computationally most expensive methods employed in the challenge. More importantly, the errors relative to experiment are much larger than the sampling errors estimated from our calculations (less than 1 kcal/mol for most molecules). Thus, there must be large systematic errors in our computational model. As will be discussed in "Dependence on the force field" section, the most likely dominating source of systematic errors is the force field employed in the simulations.

Another possible source of systematic error is the simplifications done in the simulated model system, in particular the omission of salt in the surrounding solution. The salt concentration is expected to influence the absolute binding free energies both through non-specific effects (Coulomb screening) and specific effects in the form of competitive binding of sodium ions to the host. These effects are expected to be reasonably independent of the guest molecule (and thus hardly affect the relative binding affinities), although some influence of the ligand charge (for Coulomb screening) and ligand size (for competitive binding) can be anticipated. In order to investigate this issue, we performed FM simulations including 0.3 M NaCl for two guest molecules with different charge. The results for molecule **1** and **2** are −11.5 and −10.4 kcal/mol, respectively. Remarkably, these values are within 2 kcal/mol deviation from the experimental values −9.9 and −9.6 kcal/mol. The salt effect, i.e. the difference in binding free energy between the salt-containing and saltless simulations, is practically identical for the two molecules (6.8 and 6.4 kcal/mol for **1** and **2**, respectively), despite that they have different charge (+2 and +1, respectively). However, more calculations would be needed to confirm that the salt effect is indeed independent of the ligand. Recalling that the average signed error for CGENFF is −6 kcal/mol, these results suggest that the salt effect can possibly account for the systematic shift of the binding free energies. However, as will be shown in the next section, the choice of force field also has a large effect, and more data would be needed to conclude how these effects combine.

Table 2 Binding free energies in kcal/mol for a subset of the molecules, calculated by FM using three different force fields: CGENFF, GAFF, and modified CGENFF

Mol	Exp.	CGENFF (refined)	GAFF	Mod. CGENFF
1	−9.9	−18.3 ± 0.8	−9.8 ± 0.4	−17.9 ± 0.3
6	−7.9	−18.3 ± 1.1	−10.4 ± 1.4	N/A
10	−7.9	−21.1 ± 0.4	−9.9 ± 0.9	N/A
11a	−11.1[a]	−15.7 ± 0.9	N/A	−18.6 ± 1.2
11b		−15.7 ± 3.6	N/A	−16.3 ± 0.6
12	−13.3	−11.3 ± 2.6	N/A	−12.0 ± 0.7
13	−14.1	−15.7 ± 0.5	N/A	−17.2 ± 1.2
14	−11.6	−12.2 ± 0.7	−9.8 ± 0.5	−14.5 ± 1.4

[a] Racemic mixture

Dependence on the force field

We further tested how the results depend on the choice of force field by repeating some of the simulations with the General Amber force field (GAFF) [15] and comparing the results to the corresponding CGENFF models. Due to the huge computational cost of the FM simulations and the limited time available for the SAMPL4 challenge, we only managed to run four simulations (for guests **1**, **6**, **10**, and **14**), providing a cross section of the effects one may expect for this kind of systems. The results are presented in Table 2.

The difference between the GAFF and CGENFF binding free energies is 9, 8, 11 and 2 kcal/mol, respectively, for the four considered molecules, with GAFF consistently giving less negative binding free energies. The shape of the PMFs is also affected, as shown in Fig. 5. These enormous effects of the force field are totally unexpected and clearly point at the severe problem of obtaining reliable force fields for molecules that fall outside of the general scope of biomolecular systems [32].

To validate and possibly explain the large discrepancy between GAFF and CGENFF, we analyzed the configuration

Table 3 Energy contributions (kcal/mol) to the LIE energy for molecule **6** evaluated with the CGENFF and GAFF force fields

Model	$\langle E_{ele}\rangle_{bound}$	$\langle E_{vdw}\rangle_{bound}$	$\langle E_{ele}\rangle_{free}$	$\langle E_{vdw}\rangle_{free}$	ΔE_{ele}	ΔE_{vdw}
CGENFF	−123.0 ± 1.0	−22.3 ± 0.3	−128.4 ± 0.4	−5.4 ± 0.1	5.4	−16.9
GAFF	−102.6 ± 1.1	−24.0 ± 0.3	−120.6 ± 1.2	−5.2 ± 0.3	18.0	−18.8
Difference					12.6	−2.0

The snapshots for CGENFF were obtained by filtering the FM trajectory on $|z| \leq 1$ Å and $\cos^2\theta > 0.5$ for the bound state and $10 \leq |z| \leq 20$ Å for the free state. The snapshots for GAFF were obtained by running separate unbiased MD simulations for the bound and free states

ensembles for molecule **6** in terms of the *linear interaction energy* (LIE) method [33]. In this method, the binding free energy is estimated as

$$\begin{aligned}\Delta G_{LIE} &= \alpha\Delta E_{vdw} + \beta\Delta E_{ele} \\ &= \alpha\Big(\langle E_{vdw}\rangle_{bound} - \langle E_{vdw}\rangle_{free}\Big) \\ &\quad + \beta\Big(\langle E_{ele}\rangle_{bound} - \langle E_{ele}\rangle_{free}\Big)\end{aligned} \tag{3}$$

where E_{ele} and E_{vdw} are the electrostatic and van der Waals interaction energies, respectively, between the guest and its surroundings, $\langle\rangle_{bound}$ and $\langle\rangle_{free}$ denotes averaging over the bound and free states, respectively, and α and β are constants, sometimes treated as system-specific empirical parameters. We do not assume LIE to work particularly well for estimating the absolute binding free energies for this system, but we expect it to give a reasonable estimate of the effect of changing force field.

The interaction energy contributions for the CGENFF and GAFF simulations are presented in Table 3. Both force fields give a positive electrostatic contribution to the binding due to better solvation of the polar groups in the free state. This is compensated for by a negative van der Waals contribution. Switching force field from CGENFF to GAFF gives a more positive electrostatic contribution (by 13 kcal/mol) and a more negative van der Waals contribution (by 2 kcal/mol). Using normal choices of the LIE parameters [34], such as $\alpha = 0.18$ and $\beta = 0.5$, the method predicts a difference in the binding free energy of 6 kcal/mol, i.e. rather close to the 8 kcal/mol we obtained in the FM calculations. This indicates that the main effect is related to the different partial charges of the two force fields, and suggests that the results can be improved with a careful parametrization of the electrostatic model, e.g., by fitting the charges toward high-level quantum-mechanical calculations including the effect of solvent, or by including higher-order multipoles and explicit polarizabilities.

A comparison between the GAFF results and the experimental values is shown in Fig. 9. Interestingly, the use of GAFF gives a significantly smaller AUE and AUE_o (both 1.6 kcal/mol; the CGENFF values for the same set are 8.2 and 3.8 kcal/mol, respectively). However, as can be seen in Fig. 9, the reduction of the error is mainly a trivial effect of reducing the range of the calculated free energies; in fact the GAFF estimates for these molecules are practically identical (−10 kcal/mol). In any case, the data set of four molecules is too small to draw any definitive conclusions about which force field is the better one for this problem.

Because restrained ESP (RESP) charges were employed in GAFF, the results can be used to corroborate the hypothesis that the partial charges caused the major problem. We further addressed the issue of partial charges by investigating CGENFF models with modified charges. Inspecting Table 1, we found that the predicted binding affinities for molecules **11**–**14** were too weak with the original charges; instead of being stronger binders than molecule **1** as shown by the experiment, they were all predicted to bind more weakly.

Because the binding strength is often correlated with the polarity of the ligand, we investigated how polarized the bond involving the ammonium nitrogen is for each guest. We thus computed the bond dipole moment for the bond between the ammonium nitrogen and its adjacent carbon, and compared the CGENFF bond dipole moments to those obtained from ESP charges, see Fig. 10. The ESP charges were fitted on the optimized structures of the guest molecules using the B3LYP [17, 18] functional and the 6-31G** basis set [19, 20, 21], including aqueous solvation effects with the polarizable continuum model [22] implemented in Gaussian 09 [23]. The comparison demonstrates that there is no physical reason for molecules **11**–**14** to have a smaller bond dipole moment than, e.g., molecule **5**. Therefore, we adjusted the charges based on those of molecule **5** and repeated the FM simulations with the new charges. In addition, we used a better defined molecular axis for molecules **11b** and **13**, because we had noticed a rather slow convergence for these molecules in our original results. The results are encouraging: The modified charges improve the binding energies of these molecules to the stronger side, see Table 2, column "CGENFF(modified)", and the AUE_o is slightly reduced from 3.1 to 2.9 kcal/mol among these molecules and **1**.

Another observation from Fig. 10 is that CGENFF gives a more polarized C–N bond for guest molecule **1** than for molecules **2** and **3**, whereas the ESP charges give similar bond dipole moments for the three of them. The structures

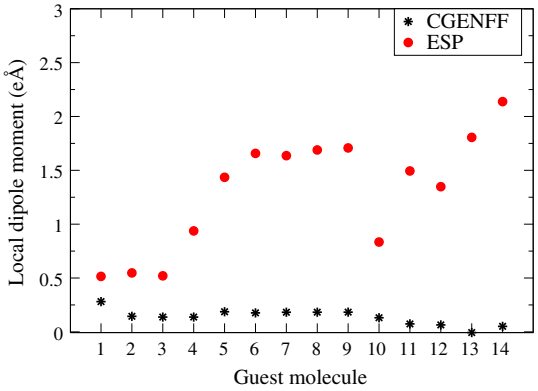

Fig. 10 Bond dipole moment for the bond from the ammonium nitrogen to its adjacent carbon. ESP charges are fitted to reproduce the electrostatic properties at the optimized structures of the guest molecules (6-31G**/B3LYP and solvated with water)

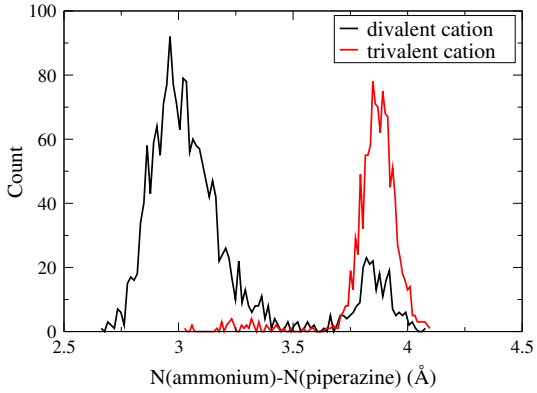

Fig. 11 Distance distribution between the ammonium nitrogen and the nearby piperazine nitrogen of guest molecule 10 using CGENFF as a divalent cation (*black curve*) and as a trivalent cation (*red curve*)

of guest molecules **1**–**3** are similar as long as the ammonium groups are concerned. We tested to model molecule **1** using more typical CGENFF charges for the primary ammonium and the methylene group. Those charges are in fact very similar to those for guest molecules **2** and **3**. However, the modification of the partial charges of molecule **1** made a negligible change to the predicted binding affinity.

Modeling guest molecule **10**

Although the protonation status of guest molecule **10** is not completely certain, we believe that the molecule is doubly protonated (divalent), based on chemical reasoning (the pK_a of the tertiary amine in the related compound 1-ethylpiperazine is 4.8 [35] and the introduction of an additional amino group would likely lower this pK_a even further) and supported by the ACD/pKa prediction. Nevertheless, the results for this molecule show some interesting features, which makes it worth investigating also the triply protonated (trivalent) compound. First, the CGENFF binding strength of the divalent compound is severly overestimated, both in absolute terms and relative to e.g. compound **1**. Second, in the PMF plot (cf. Fig. 5) of this molecule, there is only one broad binding minimum seen, in contrast to the other molecules. When manually inspecting the trajectory, the ammonium nitrogen is seen drawn to the nearby unprotonated piperazine (tertiary) nitrogen. The distance distribution between these two nitrogens, shown in black in Fig. 11, has its peak around 3 Å. As a result, the molecule assumes a perfect bidentate binding pose due to the geometry: the distance between the ammonium nitrogen and the protonated piperazine nitrogen is 5–6 Å, similar to the thickness of the host molecule, and probably thereby enhances the binding affinity.

With the trivalent model, the absolute binding energy shifts to 15.8 ± 2.1 kcal/mol, i.e. 5 kcal/mol less negative than with the divalent model. When modeled as trivalent, molecule **10** is predicted to be a weaker binder than molecule **1**, in agreement with experiment. The peak in the distance distribution between the ammonium nitrogen and the nearby piperazine nitrogen shifts to nearly 4 Å (red curve in Fig. 11), which corresponds to the length of an extended side chain of molecule **10**. However, when instead using GAFF for the divalent model, the absolute binding energy is −9.9 ± 0.9 kcal/mol, i.e. even closer to the experimental value (although with this model molecule **10** binds equally strongly as molecule **1**). In light of this observation, the alternative of modifying the CGENFF charges in the divalent model may also give a better prediction. Therefore, the more likely explanation of the anomalous results for molecule **10** is again deficiencies in the force field.

Conclusions

We have computed free energies for 14 guest molecules binding to the CB7 host by the funnel metadynamics method. We thoroughly investigated possible effects of the funnel metadynamics setup and assessed the convergence of the calculations in terms of the simulation length and the symmetry requirements imposed by this particular host–guest system. For all but two molecules, the magnitude of these sampling errors was shown to be 1 kcal/mol or less.

Despite the good statistical precision, we obtained an average unsigned error of 6.5 kcal/mol for absolute binding free energies and 3.0 kcal/mol for relative binding free energies, compared to experiment. We can conclude that there are substantial systematic errors in our model of the

system. We investigated two possible sources of errors, the neglect of salt in the solution and the use of an inaccurate force field, and found that both give significant contributions. The salt effect is in fact close to the average signed error and may account for a large part of the systematic shift. With regard to the force field, we obtained changes in binding free energies of up to 11 kcal/mol when switching from the CGENFF to the GAFF force field. For a very limited set of four molecules, the average unsigned error of the absolute binding free energies decreased to 1.6 kcal/mol, although this result may not be representative for the whole set of guest molcules. We also examined the effects of modifying the partial charges in the CGENFF force field for molecules **11**–**14**, particularly poorly predicted by the original model. The observed changes in binding strengths demonstrate the importance of the charge parametrization. Earlier investigations of similar systems have instead pointed out the importance of the van der Waals parameters [36], and, given the strong electric fields created by the charged ligands, it is also possible that an explicit account of polarization is needed. Thus, a more systematic investigation of several force fields would be needed to determine the best way of modeling this type of interactions.

Acknowledgments We thank Dr. Vittorio Limongelli for advice on the funnel metadynamics setup. This investigation has been supported by the Swedish research council (agreement C0020401).

References

1. Limongelli V, Bonomi M, Parrinello M (2013) Funnel metadynamics as accurate binding free-energy method. Proc Natl Acad Sci USA 110:6358
2. Zwanzig RW (1954) J Chem Phys 22:1420
3. Christ CD, Fox T (2014) Accuracy assessment and automation of free energy calculations for drug design. J Chem Inf Model 54:108–120
4. Hou T, Wang J, Li Y, Wang W (2011) Assessing the performance of the MM/PBSA and MM/GBSA methods. 1. The accuracy of binding free energy calculations based on molecular dynamics simulations. J Chem Inf Model 51(1):69–82
5. Warren GL, Andrews CW, Capelli AM, Clarke B, LaLonde J, Lambert MH, Lindvall M, Nevins N, Semus SF, Senger S, Tedesco G, Wall ID, Woolven JM, Peishoff CE, Head MS (2006) A critical assessment of docking programs and scoring functions. J Med Chem 49(20):5912–5931
6. Laio A, Parrinello M (2002) Proc Natl Acad Sci USA 20:12562
7. Gervasio FL, Laio A, Parrinello M (2005) Flexible docking in solution using metadynamics. J Am Chem Soc 127(8):2600–2607
8. Provasi D, Bortolato A, Filizola M (2009) Exploring molecular mechanisms of ligand recognition by opioid receptors with metadynamics. Biochemistry 48(42):10020–10029
9. Masetti M, Cavalli A, Recanatini M, Gervasio FL (2009) Exploring complex protein-ligand recognition mechanisms with coarse metadynamics. J Phys Chem B 113(14):4807–4816
10. Limongelli V, Bonomi M, Marinelli L, Gervasio FL, Cavalli A, Novellino E, Parrinello M (2010) Molecular basis of cyclooxygenase enzymes (COXs) selective inhibition. Proc Natl Acad Sci USA 107(12):5411–5416
11. Limongelli V, Marinelli L, Cosconati S, La Motta C, Sartini S, Mugnaini L, Da Settimo F, Novellino E, Parrinello M (2012) Sampling protein motion and solvent effect during ligand binding. Proc Natl Acad Sci USA 109(5):1467–1472
12. Jorgensen WL, Chandrasekhar J, Madura JD, Impey RW, Klein ML (1983) J Chem Phys 79:926
13. Humphrey W, Dalke A, Schulten K (1996) J Mol Graphics 14.1:33
14. Vanommeslaeghe K, Hatcher E, Acharya C, Kundu S, Zhong S, Shim J, Darian E, Guvench O, Lopes P, Vorobyov I, MacKerell Jr AD (2010) J Comput Chem 31:671
15. Wang J, Wolf RM, Caldwell JW, Kollman PA, Case DA (2004) Development and testing of a general AMBER force field. J Comput Chem 25(9):1157–1174
16. Bayly CI, Cieplak P, Cornell WD, Kollman PA (1993) J Phys Chem 97:10269
17. Becke AD (1993) J Chem Phys 98:5648
18. Lee C, Yang W, Parr RG (1988) Phys Rev B 37:785
19. Hehre WJ, Ditchfield R, Pople JA (1972) J Chem Phys 56:2257
20. Hariharan PC, Pople JA (1973) Theor Chem Acc 28:213
21. Francl M, Pietro W, Hehre W, Binkley JS, Defrees DJ, Pople JA, Gordon M (1982) J Chem Phys 77:3654
22. Tomasi J, Mennucci B, Cammi R (2005) Chem Rev 105:2999
23. Frisch MJ, Trucks GW, Schlegel HB, Scuseria GE, Robb MA, Cheeseman JR, Scalmani G, Barone V, Mennucci B, Petersson GA, Nakatsuji H, Caricato M, Li X, Hratchian HP, Izmaylov AF, Bloino J, Zheng G, Sonnenberg JL, Hada M, Ehara M, Toyota K, Fukuda R, Hasegawa J, Ishida M, Nakajima T, Honda Y, Kitao O, Nakai H, Vreven T, Montgomery JA Jr, Peralta JE, Ogliaro F, Bearpark M, Heyd JJ, Brothers E, Kudin KN, Staroverov VN, Kobayashi R, Normand J, Raghavachari K, Rendell A, Burant JC, Iyengar SS, Tomasi J, Cossi M, Rega N, Millam JM, Klene M, Knox JE, Cross JB, Bakken V, Adamo C, Jaramillo J, Gomperts R, Stratmann RE, Yazyev O, Austin AJ, Cammi R, Pomelli C, Ochterski JW, Martin RL, Morokuma K, Zakrzewski VG, Voth GA, Salvador P, Dannenberg JJ, Dapprich S, Daniels AD, Farkas, Foresman JB, Ortiz JV, Cioslowski J, Fox DJ (2009) Gaussian 09 Revision D.01. Gaussian Inc., Wallingford, CT
24. Phillips JC, Braun R, Wang W, Gumbart J, Tajkhorshid E, Villa E, Chipot C, Skeel RD, Kale L, Schulten K (2005) J Comput Chem 26:1781
25. Essmann U, Perera L, Berkowitz ML, Darden T, Lee H, Pedersen LG (1995) J Chem Phys 103:8577
26. Bonomi M, Branduardi D, Bussi G, Camilloni C, Provasi D, Raiteri P, Donadio D, Marinelli F, Pietrucci F, Broglia RA, Parrinello M (2009) Comp Phys Comm 180:1961
27. ACD/Labs (2013) http://www.acdlabs.com/products/percepta/predictors/pka/, Predict accurate acid/base dissociation constants from structure
28. Barducci A, Bussi G, Parrinello M (2008) Well-tempered metadynamics: a smoothly converging and tunable free-energy method. Phys Rev Lett 100(2):20603
29. Deng Y, Roux B (2009) Computations of standard binding free energies with molecular dynamics simulations. J Phys Chem B 113(8):2234–2246
30. Cao L, Isaacs L (2013) Absolute and relative binding affinity of cucurbit[7]uril towards a series of cationic guests. Supramol Chem. doi:10.1080/10610278.2013.852674
31. Liu S, Ruspic C, Mukhopadhyay P, Chakrabarti S, Zavalij PY, Isaacs L (2005) The cucurbit[n]uril family: prime components for self-sorting systems. J Am Chem Soc 127(45):15959
32. Muddana HS, Gilson MK (2012) Prediction of SAMPL3 host-guest binding affinities: evaluating the accuracy of generalized force-fields. J Comput Aided Mol Des 26(5):517–525
33. Åqvist J, Medina C, Samuelsson JE (1994) Protein Eng 7:385

34. Åqvist J, Luzhkov VB, Brandsdal BO (2002) Ligand binding affinities from MD simulations. Acc Chem Res 35:358
35. Khalili KF, Henni A, East ALL (2009) pKa values of some piperazines at (298, 303, 313, and 323) K. J Chem Eng Data 54:2914–2917
36. Moghaddam S, Yang C, Rekharsky M, Ko YH, Kim K, Inoue Y, Gilson MK (2011) New ultrahigh affinity host-guest complexes of cucurbit[7]uril with bicyclo[2.2.2]octane and adamantane guests: thermodynamic analysis and evaluation of M2 affinity calculations. J Am Chem Soc 133(10):3570–3581